# Improved Ultrasound Speckle Motion Tracking Using Nonlinear Diffusion Filtering

Abd El-Monem El-Sharkawy, Khaled Abd-Elmoniem, Abou-Bakr M. Youssef, and Yasser M. Kadah
Biomedical Engineering Dept., Cairo University, Giza, Egypt.

## ABSTRACT

In speckle motion tracking, blood velocity magnitude and direction are estimated from speckle pattern changes between successive images based on either two-dimensional correlation or sum-absolute-difference (SAD) methods. Even though these techniques have been proven useful for flow mapping applications, they suffer from bias effects in estimation due to the presence of clutter induced from structural motion. In this work, we propose a technique for reducing the clutter effect, and hence enhancing the robustness of velocity estimation. The proposed technique relies on separating the speckle from the underlying specular structures. The basic idea is to employ a speckle reduction strategy based on nonlinear coherent diffusion filtering to obtain speckle free image of vessels from an original B-mode. Then, subtracting such image from the original image, an image for speckle is obtained. Nonlinear coherent diffusion filtering has been proven successful in removing Rayleigh distributed speckle pattern resulting mainly from blood scatterers in B-mode images while preserving structural information. This allows such scattering pattern to be utilized more accurately in calculating the velocity estimates. The proposed method is applied to obtain pure speckle images in both numerical and experimental phantoms using an ultrasound research system and velocity estimates were obtained using two-dimensional correlation.

**Keywords:** Tissue Motion, Nonlinear Diffusion Filtering, 2D Speckle Tracking.

## 1. INTRODUCTION

Ultrasound imaging has become an essential diagnostic tool in many applications. Its uses extend from general imaging of anatomy to flow mapping, which makes it a versatile tool for clinical practice. Among the most promising technologies in ultrasound imaging, flow mapping offers a unique capability to visualize anatomy and assess function of the human vascular system. The anatomy is displayed in gray-scale while the blood flow velocity or power are coded in shades of red and blue to designate the direction of flow. This is the reason why this technology is termed *color flow mapping*[1].

Even though the diagnostic information content in current color flow mapping technology is high, a number of limitations exist that hinder this technology from realizing its full potential. An important example of such limitations is the absence of sufficient information about the flow direction. In particular, the exact direction of the flow is not known except for its component in only one direction representing the direction of the probe. Another limitation is the maximum velocity that can be detected with a particular pulse repetition frequency. This limitation puts an upper limit on the range of depths where color flow mapping can be used efficiently. These limitations can be shown to be a direct consequence of using the classical frequency domain methods based on the Doppler equation for velocity estimation[8].

Another class of techniques that can be used for color flow mapping that has the potential to overcome these limitations is the time-domain correlation techniques. This class of techniques relies on tracking the random pattern of scatterers in the blood between acquisitions to estimate the distance of their travel. Given the time difference between the acquisitions, this distance can be translated into an estimate of the average velocity within the volume cell of interest. This class of techniques allows the estimation of flow direction as projected onto the image plane as a by-product from the velocity estimation procedure. Moreover, the velocity estimate in this class is not directly related to the pulse repetition frequency. On the other hand, the computational complexity of this class of techniques is always demanding especially for those techniques based on 2-D cross-correlation.

An important example of the class of correlation techniques is B-mode speckle tracking. In this technique, consecutive B-mode frames are analyzed to estimate a map for the velocity variations within the ultrasound image. Hence, this technique can be useful to estimate both blood flow velocity and tissue motion. The basic idea is that the returned speckle of moving tissues is translated depending on its speed of motion in such a way that the original shape of the moving speckle is mostly retained within consecutive frames. Block matching techniques are used to estimate the projected velocity vectors of the moving speckle onto the 2-D image plane. The technique works by identifying a regular grid of kernel regions of a certain size in the first ultrasound image frame. Each kernel region is subsequently compared to all possible neighboring regions of the same size in the following frame within a predetermined search region. The size of the search region is selected to be greater than the kernel size. In general, the smaller the kernel size and the bigger the search region,

Medical Imaging 2001: Ultrasonic Imaging and Signal Processing, Michael F. Insana, K. Kirk Shung,
Editors, Proceedings of SPIE Vol. 4325 (2001) © 2001 SPIE · 1605-7422/01/$15.00

the more accurate velocity vectors are estimated. It is important to note that these methods provide vector velocity maps of very different axial and lateral resolutions. The axial resolution is significantly higher than the lateral. Consequently, the estimates for the axial component of the velocity are usually more accurate than the ones for the lateral component.

In this work, we propose a method for improving the accuracy of speckle tracking methods. Starting with a simple model for the estimation procedure, we show that the underlying structures within the blood vessel or near the vessel walls cause bias effects that might induce errors in the velocity estimates near those regions. We propose a new method that enables such bias effects to be reduced. The new method relies on separating the structures from the speckle pattern using a fast speckle reduction technique and uses the speckle-only difference image to estimate the velocity map. The proposed technique is tested on simulated and real image and its performance is analyzed.

## 2. SPECKLE TRACKING MODEL

Two main techniques are used for 2-D speckle tracking, namely, the normalized correlation algorithm and the sum-absolute-difference method. The latter method is computationally efficient and thus can be used for real-time estimation with a very close measurement accuracy to that of the first technique. The equations describing both techniques are as follows[9-12].

*Normalized Correlation Method*:

$$\rho_{m,n} = \frac{\sum_{i=1}^{k}\sum_{j=1}^{l}(x_{i,j}-\bar{x})(y_{i+m,j+n}-\bar{y})}{\sqrt{\sum_{i=1}^{k}\sum_{j=1}^{l}(x_{i,j}-\bar{x})^2\sum_{i=1}^{k}\sum_{j=1}^{l}(y_{i+m,j+n}-\bar{y})^2}} \quad (1)$$

*Sum-Absolute-Difference Method (SAD):*

$$\varepsilon_{m,n} = \sum_{i=1}^{k}\sum_{j=1}^{l}(x_{i,j}-y_{i+m,j+n}) \quad (2)$$

Here $x_{i,j}$ is the value of the gray level of pixel *(i,j)* in the kernel region of the image X, and $y_{i+m,j+n}$ is the value of the gray level of pixel ( *i+m,j+n* ) within the search region of image Y corresponding to a displacement *(m,n)*. $\bar{x}$ and $\bar{y}$ are the mean pixel values in the corresponding windows with *l* and *k* as the window dimensions. As can be observed, both methods rely on the intensity distributions of the two images in the sequence to obtain the velocity estimate. Hence, it is important to analyze the components that contribute to the intensity pattern within a vessel to properly identify their effect on the estimation process.

At first glance, we realize that structural motion resulting from wall motion or clutter (similar to what was described in classical Doppler formulations) may dramatically degrade the velocity vector estimate from speckle tracking techniques. A mathematical description of this effect can be described as follows. At the output of the beamformer and prior to the logarithmic compression stage for the envelope signal, speckle noise can be approximated as a multiplicative noise. That is,

$$f(x,y) = g(x,y)\eta_m(x,y) + \eta_a(x,y) \quad (3)$$

Here $g(x,y)$ is an unknown piecewise constant 2-D function representing the noise-free original image, $f(x,y)$ is the noisy observation of $g(x,y)$, $\eta_m$ and $\eta_a$ are multiplicative and additive noise respectively and *y* are variables of spatial locations that belong to 2-D space of all real numbers, $(x,y) \in \Re^2$ Since the effect of additive noise (such as sensor noise) is considerably small compared to that of multiplicative noise (coherent interference) , $\left(\|\eta_a(x,y)\|^2 << \|\eta_m(x,y)\|^2\right)$ Eq.(3) can be rewritten as,

$$f(x,y) \approx g(x,y)\eta_m(x,y) \quad (4)$$

The logarithmic amplification transforms the model in Eq.(4) into the classical signal in additive noise form. That is,

$$\log(f(x,y)) = \log(g(x,y)) + \log(\eta_m(x,y)) \quad (5)$$

or

$$f^l(x,y) = g^l(x,y) + \eta_a^l(x,y) \quad (6)$$

where $\eta_a^l(x, y)$ is approximated as additive white noise. We assume here that the speckle pattern has a white Gaussian noise model. This assumption is valid especially if we consider the speckle nature (initially Rayleigh scattered) after enveloping and performing logarithmic amplification on the RF signal.

In the absence of underlying structures, the speckle pattern and noise can both be assumed to have a white Gaussian noise model. In this case, any two consecutive images from the received frame sequence can be expressed as,

$$\begin{aligned} Image_1 &= S(x, y) + n_1(x, y), \\ Image_2 &= S(x - \Delta x, y - \Delta y) + n_2(x, y). \end{aligned} \tag{7}$$

Here $Image_1$ and $Image_2$ are the received consecutive image frames, S is the speckle, $n_1$ and $n_2$ are electronics produced random noise ,$x$ and $y$ are the Cartesian coordinates, while $\Delta x$ and $\Delta y$ are the displacement of the speckle pattern between the two frames. The speckle and noise are of white Gaussian noise distribution with zero means and variances $\sigma_s^2$ and $\sigma_n^2$ respectively .The cross-correlation function (Xcorr) between $Image_1$ and $Image_2$ can be computed as,

$$\begin{aligned} Xcorr(Image_1, Image_2) &= Xcorr(S(x, y), S(x - \Delta x, y - \Delta y)) + Xcorr(S(x, y), n_2(x, y)) \\ &\quad + Xcorr(n_1(x, y), S(x - x_0, y - y_0)) + Xcorr(n_1(x, y), n_2(x, y)) \\ &= \delta(x - \Delta x, y - \Delta y) + 0 + 0 + 0 \end{aligned} \tag{8}$$

This reveals that the motion can be accurately determined by estimating the peak location of the cross-correlation function. In the presence of underlying structures represented by a deterministic smooth function, $d(x, y)$, the calculations change as follows:

$$\begin{aligned} Image_1 &= S(x, y) + n_1(x, y) + d(x, y) \\ Image_2 &= S(x - \Delta x, y - \Delta y) + n_2(x, y) + d(x - \Delta x_d, y - \Delta y_d) \\ Xcorr(image_1, image_2) &= \delta(x - \Delta x, y - \Delta y) + \delta(x - \Delta x', y - \Delta y') \end{aligned} \tag{9}$$

Here $\Delta x'$ and $\Delta y'$ represent the displacement of structures. This shows that there is an ambiguity in determining the velocity vector in the presence of structural noise using template-matching techniques. In particular, when the above theoretical delta function is convolved with a smooth function that corresponds to the impulse response of the acquisition process, the actual peak of the cross-correlation function may in fact be biased towards a middle point in between the two true peaks. Since the structural motion is expected to be very small and much less than that for blood flow in general, the obtained flow velocity will be underestimated. Hence, if we can separate this deterministic component from that of the random component, the estimation accuracy of the procedure will be enhanced. This is what we will attempt to do in the following sections.

## 3. COHERENT NONLINEAR DIFFUSION FILTERING

A simple procedure to separate the speckle pattern corresponding to scatterers and random noise is to use a noise suppression (or speckle reduction) technique and obtain the difference image between the original and filtered images. The basic criteria for the speckle reduction technique for practical use in this work include edge preservation, efficient computation algorithm, and minimal need for user interaction. Among the list of possible techniques, the one based on nonlinear diffusion filtering was selected to meet all the above requirements.

Diffusion algorithms remove noise from an image by modifying the image via a partial differential equation (PDE). Consider an $m$-dimensional rectangular image domain $\Omega = (0, a_1) \times \cdots \times (0, a_m)$ with boundary $\partial\Omega$, and a gray level image, which is given by a bounded mapping $f : \Omega \to \Re$. In scale-space theory, an image is embedded into a continuous family $\{T_t f \mid t \geq 0\}$ of gradually smoother (diffused) versions of it. The original image corresponds to scale $t = 0$ and increasing the scale should simplify the image without creating spurious structures.

Consider applying the isotropic diffusion equation (the heat equation) given by $\partial I(x, y, t)/\partial t = div(c \nabla I)$, using the original degraded or noisy image $I(x, y, 0)$ as the initial condition, where $I(x, y, 0) : \Re^2 \to \Re^+$ is an image in the continuous domain, $(x,y)$ specifies spatial position, $t$ is an artificial time parameter, $c$ is the diffusion constant, and $\nabla I$ is the image gradient. Modifying the image according to this linear isotropic diffusion equation is equivalent to filtering the image with a Gaussian filter.

### 3.1. Original nonlinear diffusion formulation

Nonlinear anisotropic diffusion was first proposed to avoid blurring and localization problems of linear filtering. That is, to further encourage smoothing within a region in preference to smoothing across the boundaries[2]. The non-uniform process reduces the diffusivity at those locations having a larger likelihood to be edges, since they reveal larger gradients. A filtered image $\boldsymbol{I}(x,t)$ can be obtained as the solution of a nonlinear diffusion equation with the original image as the initial condition and reflecting boundary conditions ($\mu_1$ denotes the derivative normal to the image boundary $\partial\Omega$ ):

$$\partial_t \boldsymbol{I} = \boldsymbol{div}\left(\boldsymbol{g}\left(|\nabla \boldsymbol{I}|^2\right)\nabla \boldsymbol{I}\right) \quad on \quad \Omega\times(0,\infty), \tag{10}$$

$$\boldsymbol{I}(x,0) = \boldsymbol{f}(x) \quad on \quad \Omega, \tag{11}$$

$$\partial_n \boldsymbol{I} = 0 \quad on \quad \partial\Omega\times(0,\infty). \tag{12}$$

Eqn.(12) is the mathematical formulation of the *reflecting boundary conditions* which is also called *Neumann boundary conditions*. The *time t* is a smoothing parameter; larger values correspond to simpler (or blurred) image representations. $\boldsymbol{g}\left(|\nabla \boldsymbol{I}|^2\right)$ is the diffusivity function or the edge-stopping function[33]. This function is chosen to satisfy $\boldsymbol{g}(x)\to 0$ when $x\to\infty$ and is monotonically decreasing so that the diffusion or the smoothing decreases as the gradient strength increase and the diffusion is stopped across edges. $\boldsymbol{g}$ is a monotonically decreasing diffusivity that can take the form:

$$\boldsymbol{g}(s)=\frac{1}{1+s/\lambda^2}\quad(\lambda>0) \tag{13}$$

,

$$\boldsymbol{g}(s)=1-\boldsymbol{exp}\left(-\frac{1}{(s/\lambda)^{2n}}\right)\quad(\lambda>0) \tag{14}$$

Although $\boldsymbol{g}$(x) can be a scalar function and diffusion is still anisotropic but since $\nabla \boldsymbol{I}$ serves only as an edge detector, the applicability of the above filter is restricted to smoothing with edge enhancement. In general $\boldsymbol{g}$(x) can be in a tensor form that measures local coherence of structures such that the diffusion process become more directional in both the gradient the contour directions, the directions of maximum and minimum variations respectively.

### 3.2. Coherent Nonlinear Anisotropic Diffusion

The coherent nonlinear diffusion model takes the form,

$$\partial \boldsymbol{I}(x,y,t)/\partial t = div[D\nabla \boldsymbol{I}], \tag{15}$$

where $D\in\Re^{2\times2}$ is a symmetric positive semi-definite diffusion tensor representing the required diffusion in both gradient and contour directions and hence enhancing coherent structures as well as edges.

There are two tensors widely used to detect the local coherence; the structure tensor (also called scatter matrix or windowed second moment tensor) and the Hessian tensor which represents the second order derivatives.

$$\underbrace{\begin{pmatrix} I_x^{\,2} & I_xI_y \\ I_xI_y & I_y^{\,2}\end{pmatrix}}_{\text{Structure matrix}} \qquad \underbrace{\begin{pmatrix} I_{xx} & I_{xy} \\ I_{xy} & I_{yy}\end{pmatrix}}_{\text{Covariance (Hessian) matrix}}.$$

Because the Hessian matrix is more sensitive to noise, we preferred to use the structure tensor. The multi-scale structure matrix takes the form,

$$\begin{aligned}\boldsymbol{J}_\rho(\nabla \boldsymbol{I}) &= \boldsymbol{K}_\rho * (\nabla \boldsymbol{I}\otimes\nabla \boldsymbol{I}) \\ &= \boldsymbol{K}_\rho * (\nabla \boldsymbol{I}\cdot\nabla \boldsymbol{I}^T) \qquad (\rho\ge 0)\end{aligned},$$

or equivalently,

$$\boldsymbol{J}_\rho(\boldsymbol{I}) = \begin{pmatrix} \boldsymbol{K}_\rho * \boldsymbol{I}_x^2 & \boldsymbol{K}_\rho * (\boldsymbol{I}_x\boldsymbol{I}_y) \\ \boldsymbol{K}_\rho * (\boldsymbol{I}_x\boldsymbol{I}_y) & \boldsymbol{K}_\rho * \boldsymbol{I}_y^2\end{pmatrix}, \tag{16}$$

where,

$$K_\sigma(x) = (2\pi\sigma^2)^{-1}\cdot\exp\left(|x|^2/2\sigma^2\right).$$

The above convolution is performed component-wise mainly to average a feature over a known neighborhood (scale) where $\rho$ is the integration scale (the window size) over which the orientation information is averaged[4]. The eigenvectors

$w_1, w_2$ and the eigenvalues $\mu_1, \mu_2$ correspond to the directions of maximum and minimum variations and the strength of these variations respectively.

The formulation in (16) can be expressed as,

$$J(I) = \begin{pmatrix} w_1 & w_2 \end{pmatrix} \begin{pmatrix} \mu_1 & 0 \\ 0 & \mu_2 \end{pmatrix} \begin{pmatrix} w_1^T \\ w_2^T \end{pmatrix}. \tag{17}$$

### 3.3. Coherent diffusion for speckle reduction

The diffusion tensor $D$ should be chosen with the same eigenvectors of the structure matrix but with adaptive eigenvalues that represent the strength of diffusion in each principal direction. In particular, we used the following specifications for the diffusion tensor[5],

Let $$D(I) = \begin{pmatrix} w_1 & w_2 \end{pmatrix} \begin{pmatrix} \lambda_1 & 0 \\ 0 & \lambda_2 \end{pmatrix} \begin{pmatrix} w_1^T \\ w_2^T \end{pmatrix},$$

where, $$\lambda_1 = \begin{cases} \alpha \cdot \left(1 - (\mu_1 - \mu_2)^2 / s^2\right) & if \quad (\mu_1 - \mu_2)^2 \le s^2 \\ 0 & else \end{cases}.$$

$$\lambda_2 = \alpha \tag{18}$$

## 4. METHODS

The above filtering was applied to obtain speckle free images from the original B-mode frames. The speckle free filtered images were assumed to provide a good estimate for the deterministic structural component. Hence, the filtered images can be subtracted from the original to obtain an estimate for the speckle image. The SAD technique was applied to estimate the velocity map from the speckle images. The technique was applied to obtain flow maps for simulated and real data.

For the computer simulations, two images were generated as follows using the following steps:

1. Two vessel boundaries are generated such that they have an exponential shape in both images.
2. A structural pattern having a gaussian shape is superimposed inside the vessel of the first image and shifted slightly in the second.
3. A white Gaussian random noise is added to both image simulating electronic noise. The noise variance is $\sigma_n$ and the two noise patterns in the two images are generated independently.
4. Speckle is simulated as another white Gaussian noise pattern of variance $\sigma_s$ and was added to both images with a known shift in the speckle pattern of the two images corresponding to the displacement due to flow.

This simulation is used to test the proposed technique and to assess its performance with varying amounts of random noise. The proposed technique was also applied to estimate flow maps from real ultrasound images of a human liver.

## 5. RESULTS

Figure 1 shows the simulated blood vessel with the three components corresponding to structure, random noise and speckle. Figure 2 presents the results of applying the speckle reduction technique on the simulated image of Figure 1. This result is assumed as a good estimate for the structure in this image. The classical SAD technique was applied and compared with and without the proposed technique. As can be observed from Figures 3 and 4, the proposed technique was more robust in the areas where there is significant structure particularly near the vessel walls. The output at each small region was designated an arrow that represents the magnitude and direction of estimated flow in this area. The effect of degrading the signal-to-noise ration is shown in Figure 5. As can be seen, the proposed technique helps improve the accuracy of estimation close to that of the case when there is no structural information to bias the results.

To demonstrate the proposed technique on real data, Figure 6 shows a profile of the cross-section of a vessel near a branching site. As can be seen, the structural information is prominent in this profile and shows the validity of the proposed model. Also, the proposed technique was applied to estimate flow maps from a sequence of liver images in Figure 7 obtained from a New Sonics – Compact experimental ultrasound system (International Electronics – Biomedical Division, Egypt). The results of comparing the SAD technique with and without the proposed technique are shown in Figures 8 and 9. The estimated flow maps become more coherent when the proposed technique is applied.

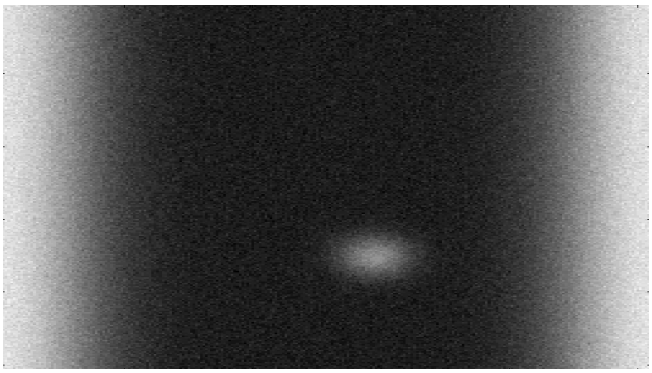

Figure 1: Simulated image consisting of scatterers, noise and underlying smooth structure.

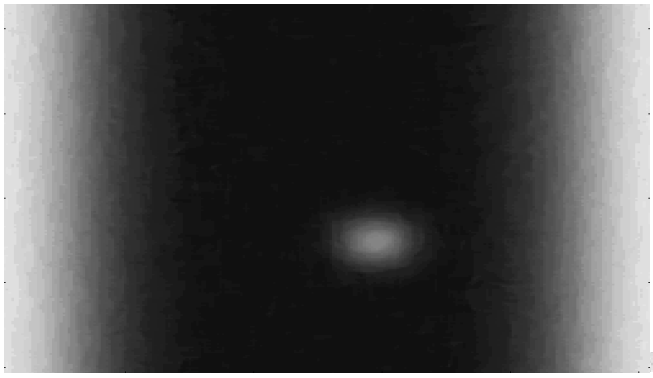

Figure 2: Filtered image showing a good approximation to the underlying structural information.

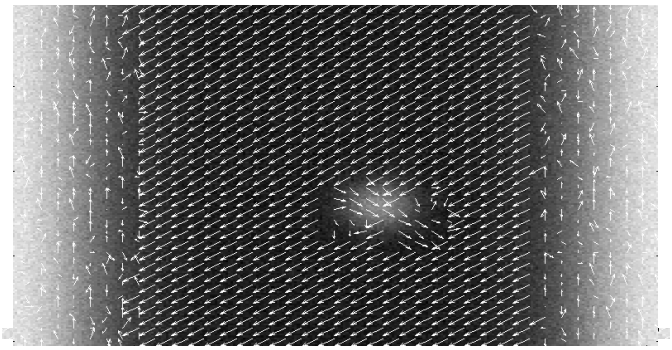

Figure 3: Estimated flow map using original images.

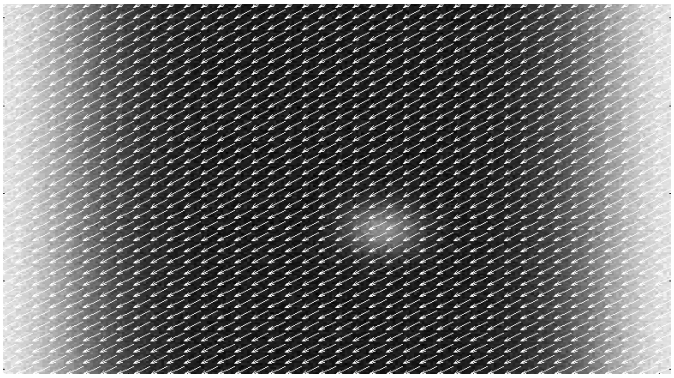

Figure 4: Estimated flow map using the proposed technique

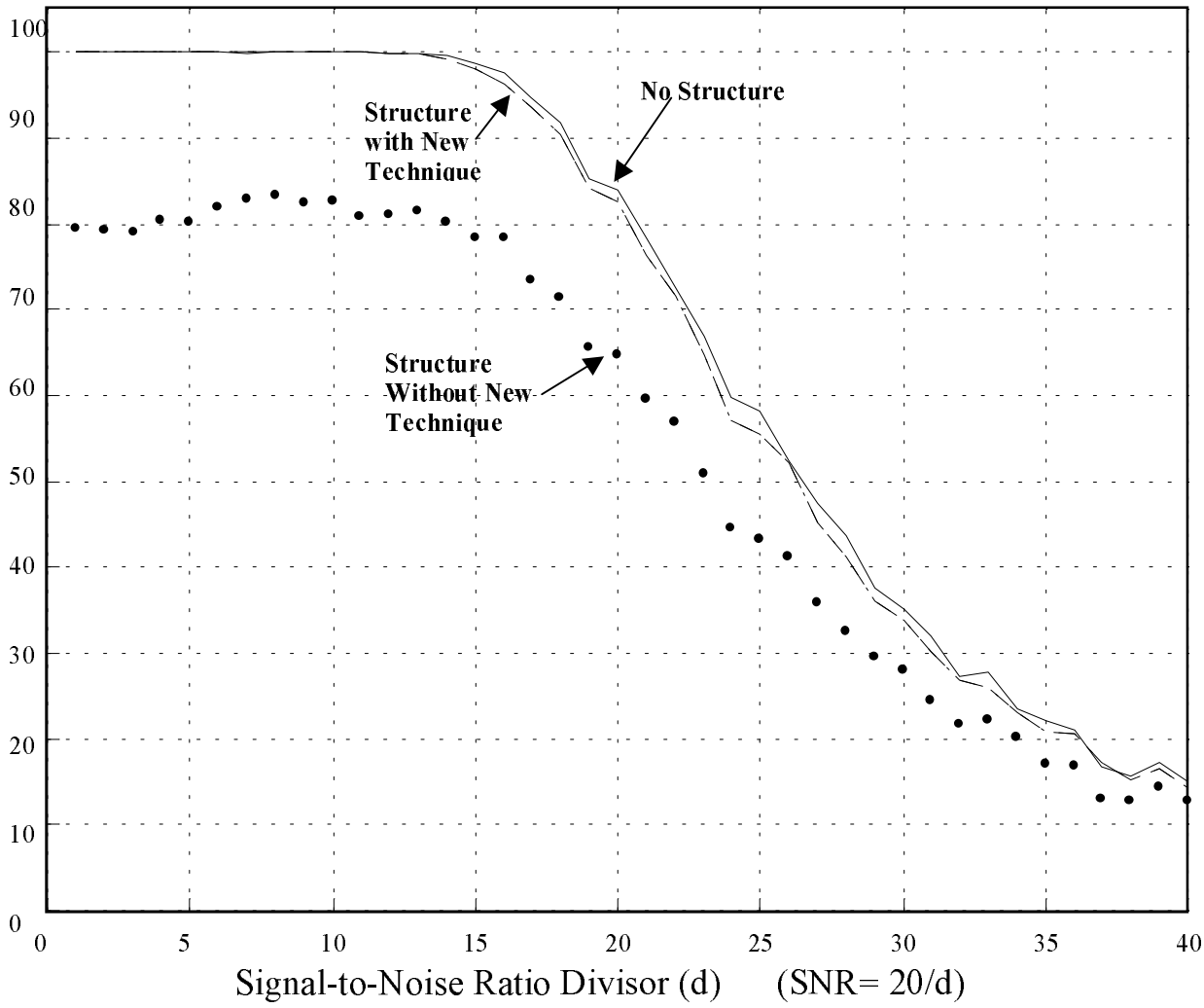


Figure 5: Evaluation of the effect of SNR on the accuracy of velocity estimation

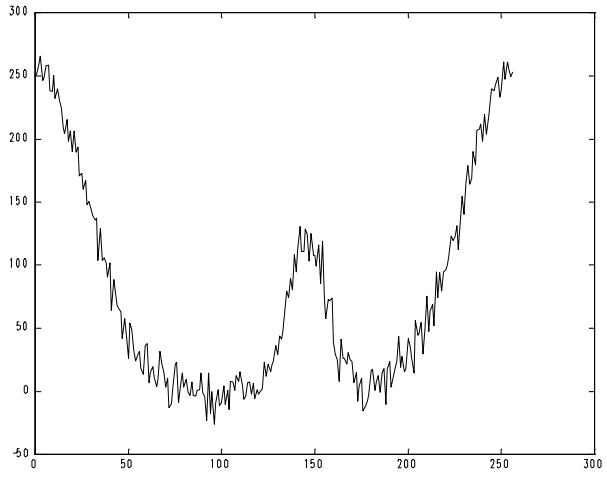


Figure 6: A cross section showing intensity distribution across a vessel showing the superimposed structural information.

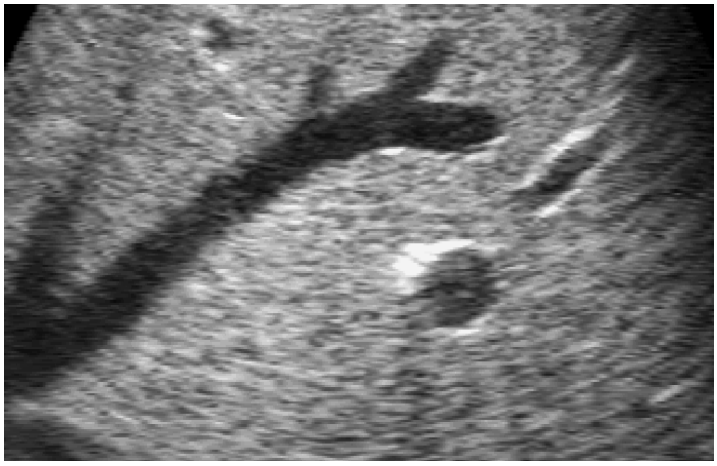

Figure 7: An image of the hepatic vein from the acquired sequence of frames

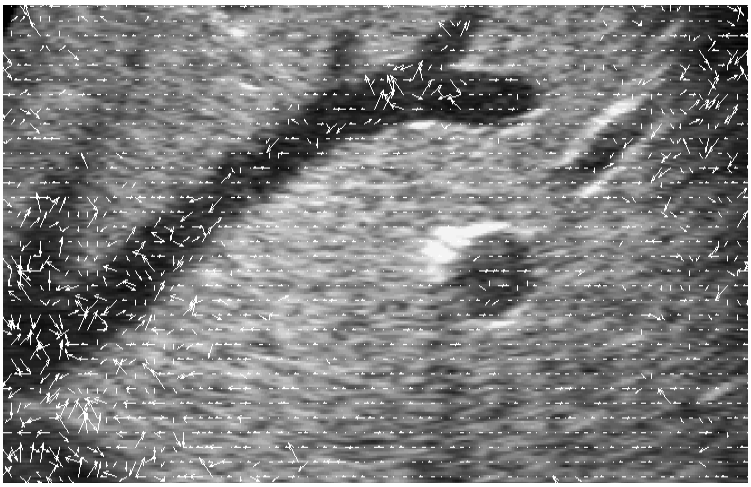

Figure 8: Velocity vectors calculated from original images

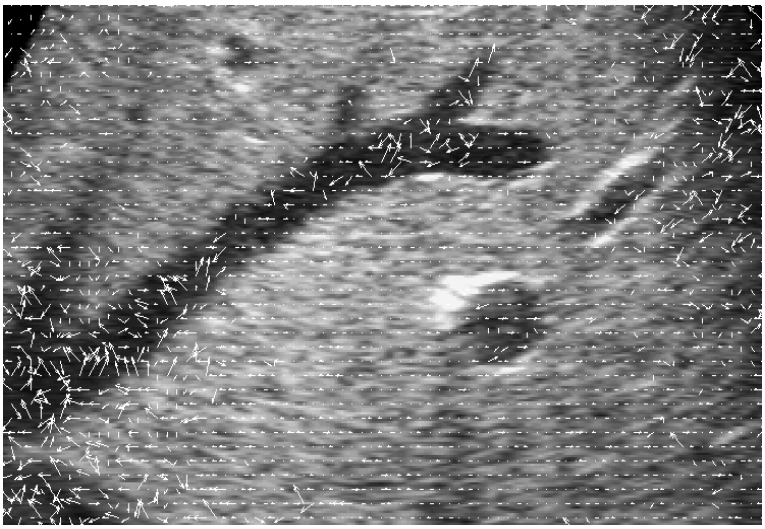

Figure 9: Velocity vectors calculated using the proposed technique

## 6. CONCLUSIONS

A new technique for improving the accuracy of velocity estimation is developed. The new technique reduces the bias effects resulting from the underlying structures. The new technique was applied on simulation as well as real ultrasound data and the results confirm the validity of this approach. Future work can be done to further develop this technique for clinical use.

## ACKNOWLEDGEMENTS

This work is partially supported by the Research and Development department of International Electronics, Biomedical division, 6 of October City, Giza, Egypt.

## 7. REFERENCES

1. Y.M. Kadah and A.H. Tewfik, "Efficient design of ultrasound true-velocity flow mapping," *IEEE Engineering in Medicine and Biology Magazine*, vol. 15, no. 5, pp. 118-125, Sept. 1996.
2. P. Perona and J. Malik, "Scale space and edge detection using anisotropic diffusion," *IEEE Trans. Patt. Anal. Mach. Intell. (PAMI)*, vol. 12, no. 7, pp. 629-639, July 1990.
3. M. J. Black, G. Sapiro, D.H. Marimont, and D. Heeger, "Robust anisotropic diffusion," *IEEE Trans. Imag. Proc.*, vol. 7, no. 3, pp. 412-432, March1998.
4. J. Weickert, "Multiscale texture enhancement," *Computer analysis of images and patterns, Lecture notes in. Comp. Science*, vol. 970, pp. 230-237, 1995.
5. K. Z. Abd-Elmoniem, Y.M. Kadah, A.-B.M. Youssef, "Real Time Adaptive Ultrasound Speckle Reduction and Coherence Enhancement," *Proc. Int. Conf. of Image Processing (ICIP-2000)*, October 2000.
6. A. K. Jain, *Fundamentals of Digital Image Processing*, Prentice-Hall, New Jersy, 1989.
7. X. Zong, A. F. Laine, and E. A. Geiser, "Speckle Reduction and Contrast Enhancement of Echocardiograms via Multiscale Nonlinear Processing," *IEEE Trans. Med. Imag.*, vol. 17, no. 4, Aug. 1998.
8. D.H. Evans and W. Norman McDicken, *Doppler Ultrasound Physics, Instrumentation and Signal Processing*, John Wiley & Sons, New York, 2000.
9. L. N. Bohs, B. J. Geiman, M. E. Anderson, S.C. Gebhart, G. E. Trahey, "Speckle tracking for multi-dimensional flow Estimation," *Ultrasonics*, vol. 38, pp. 369-375, 2000.
10. L.N. Bohs, Beth J. Geiman, K.R. Nightingale, C.D. Choi, B.H. Friemel and G.E. Trahey, "Ensemble Tracking: A New Method for 2D Vector Velocity Measurements," *IEEE 1995 International Ultrasonics Symposium* , pp. 1485-88, October 1995.
11. B.H. Friemel, L.N. Bohs, G.E. Trahey, "Relative Performance of Two-Dimensional Speckle-Tracking Techniques: Normalized Correlation, Non-Normalized Correlation and Sum-Absolute-Difference," *IEEE 1995 International Ultrasonics Symposium*, pp. 1481-84, 1995.
12. P. Munk and J.A. Jensen, "Performance of a vector velocity estimator," *IEEE 1998 International Ultrasonics Symposium,* pp. 1489-93, 1998.